Relativistic effects in angle-resolved photoemission from Cu(110)

H. Przybylski, A. Baalmann, G. Borstel, and M. Neumann
Fachbereich Physik, Universität Osnabrück, Postfach 4469,
D-4500 Osnabrück, Federal Republic of Germany
(Received 7 September 1982)

Angle-resolved normal-emission photoelectron spectra of Cu(110) are calculated within the frame of the three-step model of photoemission with spin-orbit interaction included. Corresponding experimental spectra for linearly polarized light ($\hbar\omega = 21.22$ eV) are presented and good agreement between theory and experiment is obtained. Spin-orbit coupling is important and gives rise to a detectable relaxation of single-group dipole selection rules even for materials with low atomic number. Since measured Cu(110) photoelectron spectra depend critically on the experimental angle resolution, care must be taken to separate properly this intrinsic relativistic effect from those extrinsic effects originating from finite instrumental resolution. All features in the experimental spectra may be interpreted by direct interband transitions.

I. INTRODUCTION

There has been considerable interest in angle-resolved photoemission experiments (ARPE) from single-crystal copper during the last decade.[1–18] This is primarily due to the fact that copper represents an ideal experimental and theoretical testing material for our understanding of the electronic structure of *d*-band metals. In spite of this wealth of information on copper originating so far from ARPE, the interest in this material continues and presently is focused on the following questions: (i) To which degree can bulk ARPE successfully be interpreted in terms of the direct-transition model of photoemission[19] including conservation of energy and momentum during the excitation process? (ii) Which theoretical bulk band model produces the best agreement between theory and experiment both with regard to the energetic position and the intensity of the different direct optical transitions? In practice these two problems are strongly connected since the usual procedure in interpreting ARPE is to select first all structures, which on the basis of known band-structure calculations, may be attributed to direct transitions between bulk bands, and then to look for reasonable explanations for the remaining structures.

The aim of the present contribution is to call attention to two points whose importance for ARPE on copper and their interpretation does not seem to be widely recognized. The first point is the fact that even for an element of low atomic number such as copper ($Z = 29$), the spin-orbit interaction gives rise to a relaxation of the nonrelativistic dipole selection rules[20] (NRSR), derived within the single-group formalism. As a consequence, transitions which are forbidden by NRSR may become allowed by the inclusion of spin-orbit interaction according to relativistic selection rules[21] (RSR) based on the double-group formalism and which thus show up in ARPE.[22,23] A further implication is the breakdown of the concept of parity of initial states with respect to a mirror plane, which in the past frequently has been used to determine the symmetry properties of energy bands by photoemission with unpolarized radiation.[24,25] The second point refers to the strong angular dependence of angle-resolved photoemission spectra from copper. The occurrence of this angular dependence is, of course, well known,[9,12,14] but so far it has been overlooked that it critically depends on the polarization of the incident radiation and easily may be mistaken for effects which, in fact, are due to spin-orbit interaction.[22,23]

The organization of this paper is as follows: In Sec. II we give a short account of the theoretical scheme used to calculate photoemission intensities for copper. The scheme essentially represents the relativistic version of the orthogonalized-plane-wave linearized combination of atomic orbitals (OPW-LCAO) scheme for fcc *d*-band metals originally developed by Mueller[26] and Ehrenreich and Hodges,[27] and later modified by Smith and Mattheiss.[28,29] Experimental details are described then in Sec. III. In Sec. IV both experimental and theoretical results for Cu(110) are discussed with special emphasis on those effects originating from spin-orbit interaction and the strong angular dependence of the photoemission intensities, and on the overall agreement between experiment and bulk band theory.

II. THEORETICAL PROCEDURE

The theoretical photoemission spectra are calculated neglecting surface umklapp processes from the standard expression for normal photoemission within the three-step model

$$N(E_{\rm kin},\hbar\omega)\propto\sum_{i,f}\int d^3k\,|\,\vec{A}\cdot\vec{P}_{fi}\,|^2 \times D(E_f,\vec{k})T(E_f,\vec{k})\Delta\ , \tag{1}$$

where

$$\Delta\equiv\delta(E_f-E_i-\hbar\omega)\delta(E_{\rm kin}-E_f+E_{\rm vac})\delta(\vec{k}_{||})\ .$$

Herein $E_{\rm vac}$ and $E_{\rm kin}$ denote the energy of the vacuum level and the kinetic energy of the photoelectron, respectively; $\vec{k}_{||}$ is the wave-vector component parallel to the surface, $\vec{A}$ denotes the vector potential of the electromagnetic field, and $\vec{P}_{fi}$ the vector of the momentum matrix elements between the initial states $|i\rangle$ and the final states $|f\rangle$. The transport factor $D(E_f,\vec{k})$ is assumed to be

$$D(E_f,\vec{k})=\alpha l/(1+\alpha l)\cong\alpha l\ , \tag{2}$$

where α denotes the optical-absorption coefficient and l the hot-electron mean free path. We take $l=\tau|\nabla_{\vec{k}}E_f|/\hbar$ with an assumed constant lifetime τ of the photoelectrons. The transmission factor $T(E_f,\vec{k})$ is set to zero for E_f less than $E_{\rm vac}$ and is set to

$$T(E_f,\vec{k})=\sum_{s=\pm1/2}\left|\sum_{(\vec{k}+\vec{G})_\perp>0}u^s_{f,\vec{k}+\vec{G}}\right|^2 \tag{3}$$

otherwise. This choice of $T(E_f,\vec{k})$ is suggested by the fact that the final-state wave functions $|f\rangle$ are predominantly plane-wave-like, and may be written as

$$|f\rangle=\sum_{s,\vec{G}}u^s_{f,\vec{k}+\vec{G}}\,|\,\vec{k}+\vec{G},s\,\rangle\ . \tag{4}$$

Herein $|\,\vec{k}+\vec{G},s\,\rangle$ denotes the plane-wave Pauli spinor corresponding to the reciprocal-lattice vector $\vec{G}$ and the spin state s. The coefficients $u^s_{f,\vec{k}+\vec{G}}$ as well as the momentum matrix elements P^m_{fi} ($m=x,y,z$) are calculated by the relativistic version of the OPW-LCAO scheme for fcc d-band metals.[26–29]

Conditions for the nullity of the transition matrix elements P^m_{fi} are provided by the selection rules for electric dipole transitions. For normal photoemission the final-state function $|f\rangle$ must transform according to the totally symmetric irreducible representation of the group of $\vec{k}$.[20] For photoemission along Σ in fcc crystals, allowed transitions according to NRSR are for x, $\Sigma_3\rightarrow\Sigma_1$, for y, $\Sigma_4\rightarrow\Sigma_1$, and for z, $\Sigma_1\rightarrow\Sigma_1$, where $\vec{e}=(x,y,z)$ denotes the polarization vector of the incident light with $\vec{x}||[001]$, $\vec{y}||[1\bar{1}0]$, and $\vec{z}||[110]$. Note that a transition of type $\Sigma_2\rightarrow\Sigma_1$ is strictly forbidden in NRSR. If spin-orbit interaction is taken into account, adjacent bands with different spatial symmetry Σ_i will strongly hybridize. The symmetry of all states is now Σ_5 and each spinor component in principle will contain nonzero contributions transforming as Σ_i for *all* $i=1,2,3,4$. This means that every transition along Σ will now be allowed for every direction of $\vec{e}$. The resulting RSR for x,y,z, $\Sigma_5\rightarrow\Sigma_5$, may be conveniently written in the form x, $\Sigma_5^3\rightarrow\Sigma_5^1$; y, $\Sigma_5^4\rightarrow\Sigma_5^1$; z, $\Sigma_5^1\rightarrow\Sigma_5^1$, which elucidates the role of NRSR within RSR. This form of RSR shows in the upper index which spatial symmetry Σ_i occurring in each spinor component is responsible for the nonzero transition probability of $\Sigma_5\rightarrow\Sigma_5$ in normal photoemission. Owing to the very existence of spin-orbit interaction in every material the "forbidden" transition $\Sigma_2\rightarrow\Sigma_1$ thus may show up in exact normal photoemission via hybridization of the initial-state band with adjacent bands showing different spatial symmetry.

The former argument may be easily transferred to other low-index surfaces.[21] With respect to NRSR vs RSR, normal emission along Σ is a particularly simple case since there is no spin-orbit *splitting*

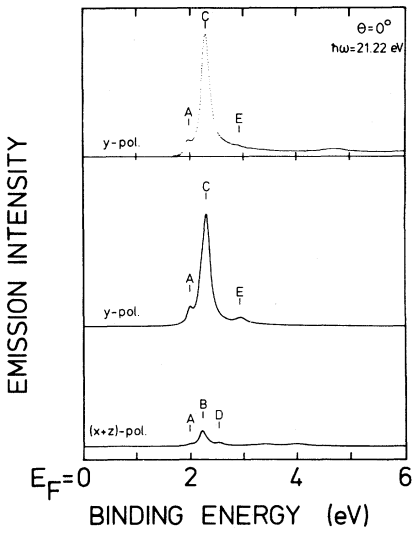

FIG. 1. Experimental (dotted line) and theoretical (solid line) normal photoemission spectra for Cu(110) excited with linearly polarized light ($\hbar\omega=21.22$ eV). For the upper two spectra the electric field vector $\vec{e}$ is parallel to $[1\bar{1}0]$ (y polarization). For the lower spectrum $\vec{e}$ is parallel to the ΓKLU plane (p polarization), the angle of incidence is 40°. Binding energies are referred to the Fermi level.

along Σ and the d-band complex exhibits an initial-state band which according to NRSR should not contribute to normal photoemission for every direction of $\vec{e}$. Thus the relaxation of NRSR may be easily studied in this configuration.

The group C_{2v} of the Σ direction in cubic crystals may also serve as an example for the fact that electronic states may no longer be characterized by their parity with respect to a mirror plane, if spin-orbit interaction is taken into account: Since there exists only one additional irreducible representation Σ_5 of the double group $\bar{C}_{2v}$, there is clearly no way to assign a definite parity to corresponding states. The same is true for the experimental configuration of mirror-plane photoemission[24,25]: Here the group of $\vec{k}$ is usually C_s, and the two additional irreducible representations Γ_3 and Γ_4 of $\bar{C}_s$ are degenerated due to time-reversal symmetry. Such photoemission experiments, therefore, will not determine any parity of the initial state with respect to a mirror plane, but at the best will provide information on the decomposition of a distinct initial state into the corresponding odd and even parts. Parity with respect to spatial inversion is, of course, not affected by spin-orbit interaction.

III. EXPERIMENTAL DETAILS

The Cu(110) specimen was mechanically polished after spark cutting from a single crystal. It was cleaned by ion bombardment (600 eV) and afterwards annealed up to 700 °C. The ultraviolet photoemission spectroscopy (UPS) measurements were carried out in a magnetic shielded (<10 mG) ultrahigh vacuum chamber with base pressure less than 1×10^{-10} mbar. This chamber was equipped with low-energy electron diffraction and Auger facilities, an uv light source, and a movable electron-energy analyzer to perform UPS experiments. By the electron-energy analyzer electrons within an acceptance angle of $\pm1.5°$ were collected. With a constant pass energy of the analyzer the resolution in energy was 150 meV or better. A capillary discharge lamp was used to produce uv light. By a three-mirror reflecting system, which could be moved into the light path, the light was polarized to a degree of more than 90%.

IV. RESULTS AND DISCUSSION

In Figs. 1 and 2 we show both theoretical and experimental normal photoemission spectra for Cu(110). The angle of incidence for the light ($\hbar\omega=21.22$ eV) was chosen to be 40°. The light wave was linearly polarized with its polarization vector $\vec{e}$ lying in the ΓKLU and ΓKWX crystal plane, respectively. The theoretical spectra have been calculated by the procedure outlined in Sec. II for parameters of the OPW-LCAO scheme as given by Smith.[29,30] Lifetime-broadening effects have been taken into account by convoluting the distribution of N with a Lorentzian assuming a full width at half maximum (FWHM) equal to $\lambda(E_i-E_F)^2$ with $\lambda=0.05$ eV^{-1} (E_F is the Fermi energy). The screened electromagnetic field $\vec{A}$ inside the sample was calculated according to the classical Fresnel for-

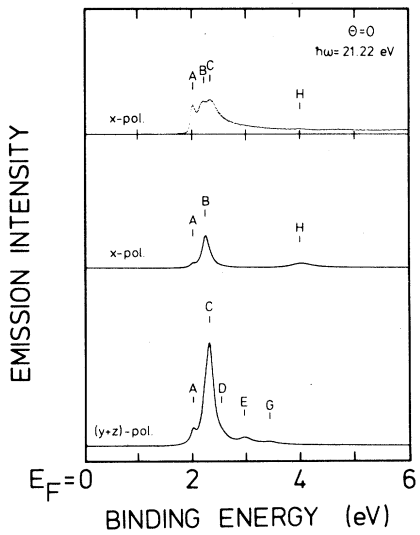

FIG. 2. Experimental (dotted line) and theoretical (solid line) normal photoemission spectra for Cu(110) excited with linearly polarized light ($\hbar\omega=21.22$ eV). For the upper two spectra the electric field vector $\vec{e}$ is parallel to [001] (x polarization). For the lower spectrum $\vec{e}$ is parallel to the ΓKWX plane (p polarization), the angle of incidence is 40°. Binding energies are referred to the Fermi level.

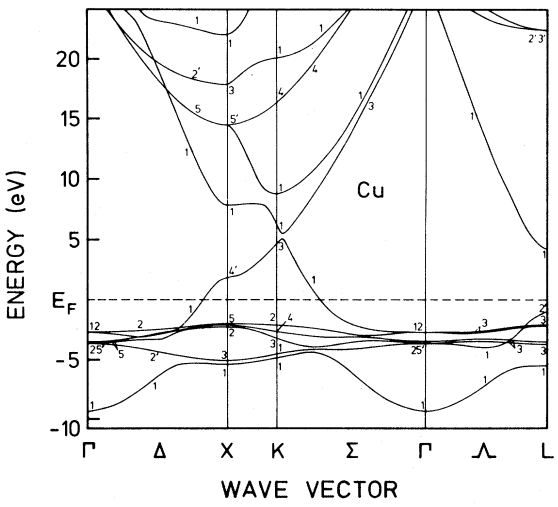

FIG. 3. Band structure of copper.

TABLE I. Comparison of experimental and theoretical data for normal photoemission from Cu(110) for $\hbar\omega = 21.22$ eV.

	Transitions $\Sigma_5^i \rightarrow \Sigma_5^1$	Binding energies below Fermi level ($-E_B$/eV) Theory	This experiment	Ref. 13	Ref. 22
A	$i=2$	1.98	2.03	2.02	2.01
B	$i=3$	2.21	2.20		2.15
C	$i=4$	2.30	2.29	2.33	2.33
D	$i=1$	2.53	2.57		
E	$i=4$	2.94	2.88	2.89	2.9
F	$i=2$	3.11	3.13	3.19	
G	$i=1$	3.40	3.46		
H	$i=3$	3.99	3.92	4.04	4.0
I			4.73	4.80	4.8
K			5.15	5.20	5.2

mulas from optical constants published by Hagemann *et al.*[31]

The band structure of Cu is shown in Fig. 3. Owing to crystal anisotropy the *d*-band complex (bands 2–6) is totally split along Σ according to $d \rightarrow 2\Sigma_1 + \Sigma_2 + \Sigma_3 + \Sigma_4$. For an excitation energy $\hbar\omega = 21.22$ eV, two bands with symmetry Σ_1 may serve as final-state bands in normal photoemission, namely band 10 for $\vec{k}$ close to X and band 8 for $\vec{k}$ in the interval ΓK. Altogether, for $\hbar\omega = 21.22$ eV, there are eight transitions A–H from *d* bands energetically possible, which have been listed in Table I. The corresponding final-state band is band 10 in the case A–C and band 8 for D–H.

Within an empty lattice, band 8 along ΓK has the plane-wave decomposition $|\vec{k}_{\bar{1}\bar{1}1}\rangle + |\vec{k}_{\bar{1}\bar{1}\bar{1}}\rangle$, whereas band 10 close to X consists of plane waves $|\vec{k}_{\bar{2}00}\rangle + |\vec{k}_{0\bar{2}0}\rangle$ ($\vec{k}_{lmn} \equiv \vec{k} + \vec{G}_{lmn}$). Thus for zero effective potential, emission from these two bands does not correspond to primary-cone emission. But it turns out that the actual effective crystal potential results in a strong hybridization of the bands 10 ($\Sigma_1 \rightarrow X_3$) and 11 ($\Sigma_1 \rightarrow X_1$) near X by means of lifting the accidental degeneracy of X_3 and X_1 in the empty lattice. Since band 11 is of type $|\vec{k}_{\bar{2}\bar{2}0}\rangle$ and thus gives rise to primary-cone emission, this means that band 10 near X may also contribute significantly in primary-cone emission. The calculated leading plane-wave terms at $\vec{k} = (\pi/4a)$ (770) in band 10 are, in fact, $0.63(|\vec{k}_{\bar{2}00}\rangle + |\vec{k}_{0\bar{2}0}\rangle) - 0.40\,|\vec{k}_{\bar{2}\bar{2}0}\rangle$, which clearly shows this Σ_1-Σ_1 hybridization mechanism due to the actual effective Cu potential. For band 8 along ΓK, similar arguments do not hold and consequently the transitions D–H occur with very low intensity compared to that of A–C.

In the following we will first discuss the more intense transitions A–C close to the X point. The spectra in Fig. 1 correspond to linear polarization $\vec{y} \| [1\bar{1}0]$ for *s* polarization and of type $x+z$ for *p* polarization. According to NRSR we thus expect only transition C to occur for *s* polarization and only transition B for *p* polarization. In particular, the transition A should not show up in the spectra since it is strictly forbidden by NRSR. It, nevertheless, appears clearly for *s* polarization in both the experimental and the theoretical spectrum, thus proving the failure of NRSR even for elements with low atomic number. In contrast to A, the transitions B and C seem to behave according to NRSR, but this impression is only due to the very small energetic separation ($\Delta E \cong 0.1$ eV) between B and C which does not allow for a clear resolution of both peaks. If the spectrum for *s* polarization is recalculated with FWHM = 0.05 eV, both B and C are clearly seen.[23] The occurrence of A and B for excitation with *s*-polarized light in Fig. 1 has its origin in the hybridization of the corresponding Σ_2 and Σ_3 initial-state bands with the adjacent Σ_4 band close to X. The spectra in Fig. 2 yield essentially the same results. Here *s* polarization corresponds to linear polarization $\vec{x} \| [001]$ and *p* polarization to $y+z$. The occurrence of transition A in all spectra of Fig. 2 is due to hybridization of the Σ_2 band with the adjacent Σ_3 (Σ_4) band in the case of *s* polarization (*p* polarization). Again a higher energetic resolution of the main peak in Fig. 2 would reveal that it, in fact, consists of both transitions B and C.

The agreement between the theoretical and experimental photoemission spectrum for excitation with *s*-polarized light is much better in Fig. 1 than in Fig. 2. The reason for this fact is that the relative intensity of the peak A is extremely sensitive to slight variations of the direction of $\vec{k}$ near the direction Σ, if the exciting light shows *x* polarization. This mechanism will give rise to a strong dependence of the measured relative intensities on the effective ac-

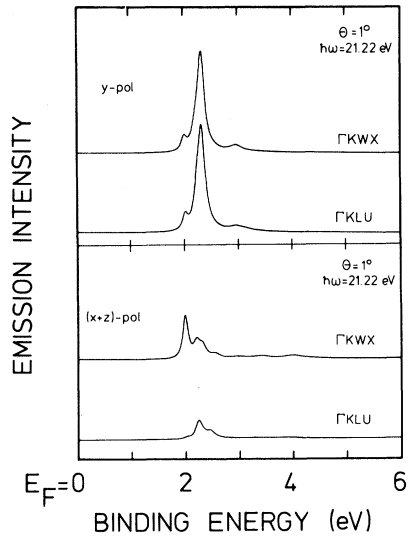

FIG. 4. Theoretical photoemission spectra for Cu(110) for s-polarized light (upper part) and p-polarized light (lower part). Electron emission is 1° off the exact surface normal in the ΓKWX or ΓKLU plane as indicated. The plane of incidence of the light ($\hbar\omega = 21.22$ eV) is the ΓKLU plane, the angle of incidence is 40°.

ceptance angle of the analyzer if the electromagnetic field component A_x is nonzero.

To demonstrate this strong angular dependence we show in Fig. 4 calculated Cu(110) photoemission spectra for $\vec{e}$ lying in the ΓKLU plane and electron emission, which is 1° off the exact surface normal in the ΓKWX and ΓKLU crystal plane, respectively. If one compares the spectra in Fig. 4 and Fig. 1, one finds no significant angular effect in the relative intensities for s-polarized light, but rather drastic effects for excitation with p-polarized light and electron emission within the ΓKWX plane. The effect becomes even more clear if $\vec{e}$ is changed to lie in the ΓKWX plane. The corresponding spectra are shown in Fig. 5 for off-normal electron emission in the ΓKWX and ΓKLU plane, respectively. The comparison of Fig. 5 and Fig. 2 now yields immediately that it is the s component A_x of the electromagnetic field $\vec{A}$ parallel to the ΓKWX plane, which is responsible for the pronounced angular effect, and that this strong effect occurs only for those photoelectrons emitted in the ΓKWX plane. The initial-energy plane in $\vec{k}$ space, defined by $E_f(\vec{k}) - E_i(\vec{k}) = \hbar\omega$, is, therefore, highly anisotropic near X in the sense that the degree of hybridization of Σ_2 and Σ_3 states strongly varies near Σ in the ΓKWX plane, but remains nearly constant in the ΓKLU plane.

These theoretical predictions concerning the angular dependence of the Cu(110) photoemission spectra are completely corroborated by the experimental data shown in Fig. 6. Both series of spectra corre-

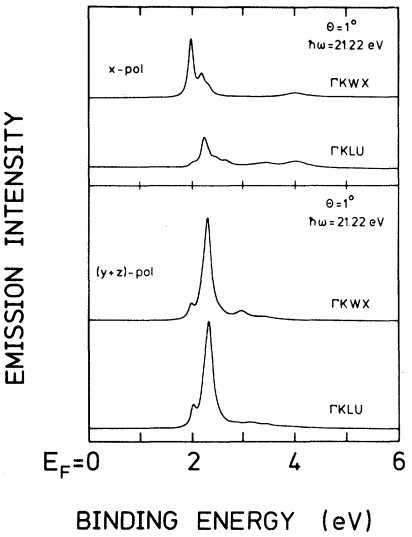

FIG. 5. Theoretical photoemission spectra for Cu(110) for s-polarized light (upper part) and p-polarized light (lower part). Electron emission is 1° off the exact surface normal in the ΓKWX or ΓKLU plane as indicated. The plane of incidence of the light ($\hbar\omega = 21.22$ eV) is the ΓKWX plane, the angle of incidence is 40°.

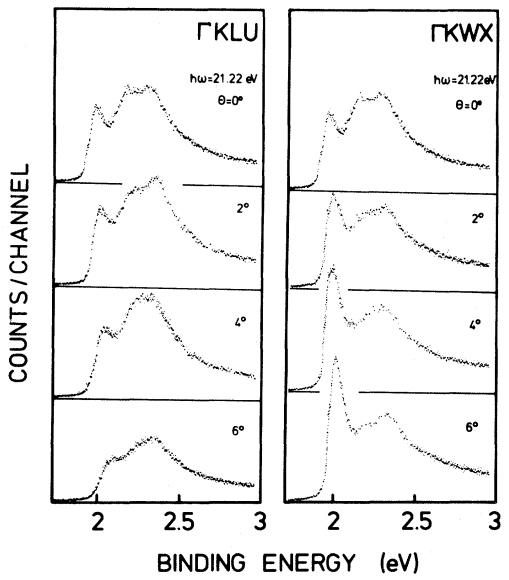

FIG. 6. Experimental photoemission spectra for Cu(110) excited with s-polarized light ($\hbar\omega = 21.22$ eV). The electric field vector $\vec{e}$ is parallel to [001] (x polarization). Electron emission is analyzed off normal by an angle θ in the ΓKWX and ΓKLU plane as indicated.

spond to excitation with s-polarized light in the ΓKWX plane, i.e., $\vec{e}$ along $\vec{x}||[001]$. It is seen that in the case of off-normal emission in the ΓKLU plane, the relative intensities stay nearly constant up to 4° and then decrease. For emission in the ΓKWX plane, on the other hand, the intensity of peak A increases drastically with increasing emission angle. These results clearly demonstrate that in normal photoemission from Cu(110), pure external instrumental effects due to angle resolution, acceptance angle of the analyzer, and degree of light polarization may easily mask intrinsic effects in the electronic structure of the sample and must be taken into account correctly, in order to avoid errors in the interpretation of experimental data.

We now turn to a discussion of the low-intensity transitions D—H. The small intensity of these transitions, when compared to that of A—C, is due to secondary-cone emission and makes their experimental observation in photoemission with polarized light very difficult.[32] But for excitation with unpolarized light the different transitions may be clearly identified, as demonstrated in Fig. 7 for $\hbar\omega = 21.22$ eV. Figure 7 shows in the upper part the complete experimental spectrum and in the lower part that spectrum which is obtained after subtracting the most intense peak C according to a Lorentz distribution. The transitions D—H clearly show up in Fig. 7 and demonstrate that all direct transitions, which are expected on the basis of the band structure in Fig. 3, in fact do occur in the experimental spectra. The agreement between theoretical and experimental binding energies for A—H according to Table I is excellent and shows that the underlying bulk band model is basically correct. There is no indication that density-of-states arguments play any significant role for the observed features A—H.

There are two peaks in Fig. 7 which may not be explained by direct transitions between bulk bands calculated for the ground-state potential of solid Cu. These features occur at a binding energy of 4.73 and 5.15 eV, respectively. They may be interpreted as transitions into evanescent band-gap states,[9] i.e., states which decay towards the solid and propagate on the vacuum side. Nilsson and Dahlbäck[11] have pointed out that the occurrence of such transitions may be explained by the damping of the excited states, which makes the band gap disappear and gives rise to bands with a free-electron-like behavior within the gap. In this context emission from evanescent band-gap states must be interpreted as an excited-state effect which critically depends on the finiteness of the electron and hole lifetime, and, therefore, cannot be directly related to usual ground-state band calculations. In a strict sense this reservation holds for all photoemission data, since in

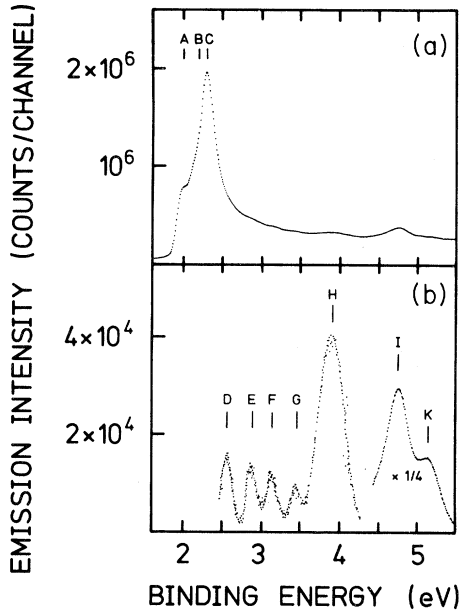

FIG. 7. (a) Normal-emission photoelectron spectrum of Cu(110) excited with unpolarized light ($\hbar\omega = 21.22$ eV) with a high signal-to-noise ratio. (b) Peak C together with a constant background has been subtracted from the spectrum shown in (a) in order to detect the low-intensity peaks.

order to measure the binding energy and the wave vector of an electron, it must be excited out of the ground state. But the results of this work as well as those of many other authors in this field show that most of the photoemission data in the uv spectral region may, in fact, be understood on the basis of ground-state properties of the solid. Nevertheless, the general problem remains, how to take into account final-state corrections in order to correlate experiment and theory in a more rigorous way.

V. SUMMARY

From a comparison of theoretical and experimental photoemission spectra for Cu(110) we have found that all ten experimental features A—K occurring in normal emission for $\hbar\omega = 21.22$ eV may be attributed to direct interband transitions along Σ within a ground-state band structure (A—H) or a self-energy-corrected band structure (I,K). There is no indication that density-of-states transitions play any significant role for Cu(110).

For the peaks A—H, corresponding to direct transitions within the ground-state band structure, the agreement between experimental and theoretical spectra (calculated relativistically within the three-step model) is very good, both with regard to the energetic positions and the strengths of the transitions. The large observed and calculated intensity of the

transitions $A-C$, when compared to that of $D-H$, shows that the distinction of primary- and secondary-cone photoemission may break down completely in those cases, where the actual varying crystal potential induces strong hybridization between bands showing the same spatial symmetry.

Spin-orbit interaction plays an important role for Cu(110) by mixing different spatial symmetries for adjacent initial-state bands. This in turn changes the dipole selection rules and gives rise to the occurrence of forbidden transitions. The importance of this effect, even for low-Z materials, may be judged from the observation that in the case of Cu(110), the emission intensity due to transition A clearly exceeds that originating from evanescent band-gap states (I,K) and true secondary-cone emission ($D-H$).

Great experimental care must be taken not to confuse this intrinsic effect due to spin-orbit interaction with extrinsic effects originating from finite experimental resolution. In this regard for Cu(110) the most critical experimental parameter turns out to be the acceptance angle of the analyzer.

ACKNOWLEDGMENT

Support by the Bundesministerium für Forschung und Technologie is gratefully acknowledged.

[1]U. Gerhardt and E. Dietz, Phys. Rev. Lett. 26, 1477 (1971).
[2]H. Becker, E. Dietz, U. Gerhardt, and H. Angermüller, Phys. Rev. B 12, 2084 (1975).
[3]P. O. Gartland and B. J. Slagsvold, Phys. Rev. B 12, 4047 (1975).
[4]L. Ilver and P. O. Nilsson, Solid State Commun. 18, 677 (1976).
[5]J. Stöhr, G. Apai, P. S. Wehner, F. R. McFeely, R. S. Williams, and D. A. Shirley, Phys. Rev. B 14, 5144 (1976).
[6]R. S. Williams, P. S. Wehner, J. Stöhr, and D. A. Shirley, Phys. Rev. Lett. 39, 302 (1977).
[7]J. Stöhr, P. S. Wehner, R. S. Williams, G. Apai, and D. A. Shirley, Phys. Rev. B 17, 587 (1978).
[8]E. Dietz and D. E. Eastman, Phys. Rev. Lett. 41, 1674 (1978).
[9]E. Dietz and F. J. Himpsel, Solid State Commun. 30, 235 (1979).
[10]J. A. Knapp, F. J. Himpsel, and D. E. Eastman, Phys. Rev. B 19, 4952 (1979).
[11]P. O. Nilsson and N. Dahlbäck, Solid State Commun. 29, 303 (1979).
[12]P. Thiry, D. Chandesris, J. Lecante, C. Guillot, R. Pinchaux, and Y. Petroff, Phys. Rev. Lett. 43, 82 (1979).
[13]R. Courths, S. Hüfner, and H. Schulz, Z. Phys. B 35, 107 (1979).
[14]D. Westphal, D. Spanjaard, and A. Goldmann, J. Phys. C 13, 1361 (1980).
[15]M. Lindroos, H. Asonen, M. Pessa, and N. V. Smith, Solid State Commun. 39, 285 (1981).
[16]R. Courths, V. Bachelier, B. Cord, and S. Hüfner, Solid State Commun. 40, 1059 (1981).
[17]M. Pessa, M. Lindroos, H. Asonen, and N. V. Smith, Phys. Rev. B 25, 738 (1982).
[18]R. Courths, Solid State Commun. 40, 529 (1981).
[19]C. N. Berglund and W. E. Spicer, Phys. Rev. 136, A1030 (1964).
[20]J. Hermanson, Solid State Commun. 22, 9 (1977).
[21]G. Borstel, W. Braun, M. Neumann, and G. Seitz, Phys. Status Solidi B 95, 453 (1979); G. Borstel, M. Neumann, and M. Wöhlecke, Phys. Rev. B 23, 3121 (1981).
[22]A. Goldmann, D. Westphal, and R. Courths, Phys. Rev. B 25, 2000 (1982).
[23]G. Borstel, H. Przybylski, M. Neumann, and M. Wöhlecke, Phys. Rev. B 25, 2006 (1982).
[24]N. V. Richardson and J. K. Sass, J. Phys. F 8, L99 (1978).
[25]N. V. Richardson, D. R. Lloyd, and C. M. Quinn, J. Electron Spectrosc. Relat. Phenom. 15, 177 (1979).
[26]F. U. Mueller, Phys. Rev. 153, 659 (1967).
[27]H. Ehrenreich and L. Hodges, in *Methods in Computational Physics,* edited by B. Alder, S. Fernbach, and M. Rotenburg (Academic, New York, 1968), Vol. 8, p. 149.
[28]N. V. Smith and L. F. Mattheiss, Phys. Rev. B 9, 1341 (1974).
[29]N. V. Smith, Phys. Rev. B 19, 5019 (1979).
[30]The Cu parameters according to Ref. 29 have been modified with respect to the Fletcher-Wohlfahrt parameters A_4 and A_5 as described in Ref. 23. For the spin-orbit coupling parameter ξ_{3d} a value of 0.08 eV was used.
[31]H. J. Hagemann, W. Gudat, and C. Kunz, DESY Report No. SR-74/7 (unpublished); J. Opt. Soc. Am. 65, 742 (1975).
[32]According to the experimental spectra in Figs. 1 and 2, peak E occurs primarily for y polarization and peak H for x polarization. This is in full agreement with theory.